

## TURBINE STAGE MASS FLOW EVALUATION IN A COMPRESSION TUBE FACILITY

L. Porreca    R. Dénos  
von Karman Institute for Fluid Dynamics  
Chaussée de Waterloo, 72  
1640 Rhode Saint Genèse, Belgium  
contact: denos@vki.ac.be

### ABSTRACT

This paper describes a procedure to determine the mass flow of a cooled turbine stage tested in a compression tube facility. In this type of test rig, high-pressure air pushes a lightweight piston inside a closed cylinder. A quasi-isentropic compression is performed. Then, a shutter valve is opened, the flow enters the settling chamber, chokes the downstream throat and fills up the downstream vacuum tank.

Thanks to mass flow and energy balances, pressure and temperature history can be predicted in all the elements of the facility and the mass flow can be evaluated in key locations.

The model is validated against a large number of test data and is able to determine the mass flow for each single test. Two different turbine configurations are investigated and single test uncertainties of 0.88 % and 1.6 % are achieved, depending on the test condition.

### NOMENCLATURE

$A$	area
$c_v$	specific heat at constant volume
$c_p$	specific heat at constant pressure
$h$	enthalpy
$m$	mass
$\dot{m}$	mass flow
$P$	pressure
$R$	perfect gas constant
$T$	total temperature
$t$	time
$u$	internal energy
$V$	volume
<u>Greek</u>	
$\gamma$	isentropic exponent
$\rho$	density
$\eta$	turbine stage efficiency
$\pi$	turbine stage total to total pressure ratio

### Subscripts/superscripts

1	volume 1 in the compression tube
2	volume 2 in the compression tube
3	settling chamber
4	dump tank
Cool	coolant flow
ex	rotor exit conditions
i	time step
in	inlet compression tube
ini	initial value
Leak	leakage flow
out	outlet compression tube
S	Sonic throat
s	static quantity
tot	total
V	Vent hole

### INTRODUCTION

Short duration turbomachinery test facilities offer the potential of testing components under engine representative conditions at low cost. On the other hand, due to the short test time (typically 0.2 to 0.5 s), measuring accurately detailed flow quantities is a difficult task and special instrumentation with adequate response time must be utilized.

The accurate measurement of overall quantities like power, mass flow or efficiency is even more difficult owing to the necessity of acquiring simultaneously a number of quantities in a very short time.

In particular, the stage mass flow is usually calculated from pressure measurements across a calibrated orifice located downstream of the stage (Keogh et al., 2000), using the time history of the pressure decay in the supply tank (Guenette et al., 1989) or by temperature, pressure and velocity traverses across a well-known section. These techniques are not adequate for a compression tube facility.

This paper describes a novel mass flow measurement method specific to this type of test rig.

The operating principle of the rig is described and details on the turbine stage are given.

Then, a modelisation of each element of the rig is carried out. It is based on mass and energy balances.

Total pressure and temperature histories are predicted and compared with experimental data in a number of locations and for several test conditions. The mass flow is computed in two locations: at the vent hole and at the downstream sonic throat.

Finally, an uncertainty analysis is carried out and the method is applied to a number of tests to demonstrate its effectiveness and accuracy.

### THE VKI CT-3 FACILITY

The VKI CT-3 facility is a short duration turbine test rig that operates under the principle of the isentropic light piston compression tube developed at the University of Oxford by Jones et al., 1973. The Reynolds and Mach numbers, the gas to wall and the gas to coolant temperature ratios can be reproduced and adjusted independently within a range that is representative of high-pressure turbine operation in modern aero-engines.

The facility consists of a large compression tube, a settling chamber, a test section and a dump tank as shown in Figure 1.

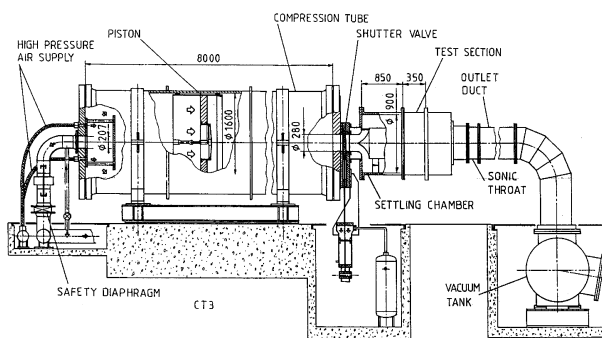


Figure 1: The VKI CT3 compression tube facility.

High-pressure air pushes a free-moving light weight piston in the upstream cylindrical reservoir. Downstream of the piston, the air is compressed in a quasi-isentropic way. During this phase, the other extremity of the tube remains closed thanks to a vertical oriented fast opening shutter valve that secures the central vent hole. When the wanted levels of pressure and temperature are reached downstream of the piston, the shutter valve opens quickly. The air is discharged in the settling chamber and the test section. After a short transient, the downstream

throat becomes choked and maintains constant flow properties in the test section. The pressure in the downstream dump tank, that was initially under vacuum, increases. The test conditions remain constant until the piston reaches the extremity of the tube or until the downstream throat becomes unchoked. Typical testing times range between 0.2 and 0.5 s. Full details on the CT3 compression tube facility are reported by Sieverding and Arts, 1992.

### THE TRANSONIC AXIAL TURBINE STAGE

The transonic axial high-pressure turbine stage under investigation is representative of a wide class of aero-propulsion engines.

The stator is internally cooled with air at ambient temperature resulting in a gas to coolant temperature ratio of 1.5. The coolant air is ejected through a slot in the trailing edge and represents 3% of the overall stage mass flow. Air can also leak or enter the test section through a small gap located between the stator and the rotor platforms at hub.

Detailed investigations were carried out previously focusing on the time-averaged and time-resolved aero-thermal flow in the stage. Further details on these investigations and on the stage geometry can be found in Dénos et al., 2001.

Two different test rig configurations have been investigated: single stage and 1 and ½ stage.

In the single stage configuration, the stage pressure ratio was varied (see Table 1). In this case, the rotor was equipped with uncooled blades.

In the 1 and ½ stage configuration, the Reynolds number was increased by 25% and the rotor is film cooled with a coolant mass flow rate of 0.5% or 0.78% depending on the test conditions. All tests are performed at 6500 RPM. In the following, the test conditions will be referred to as indicated in column 1 of Table 1.

Single stage configuration				
Test conditions	Re	$P_0$ (bar)	$T_0$ (K)	$P/p$
Re nom, P/p nom	$1.01 \cdot 10^6$	1.62	440	3.04
Re nom, P/p low	$0.99 \cdot 10^6$	1.62	440	2.32
1 and ½ stage configuration				
Re high, P/p nom	$1.26 \cdot 10^6$	2.22	480	3.08
0% cooling	no rotor coolant flow			
2% cooling	0.5 % of stage mass flow			
3% cooling	0.78 % of stage mass flow			

Table 1: Operating conditions (Reynolds number is based on the blade chord and the stator exit conditions).

## MODELISATION OF THE COMPRESSION TUBE FACILITY

### Compression phase

Prior to the compression, a well-defined initial pressure level is set in the upstream tube. It is calculated as a function on the wanted final levels of pressure and temperature at the end of the compression, i.e. stage inlet conditions, and as a function of the initial air temperature inside the tube (a priori ambient temperature):

$$\frac{P_{ini}}{P_{fin}} = \left( \frac{T_{ini}}{T_{fin}} \right)^{\frac{\gamma}{\gamma-1}}$$

These initial conditions together with the initial piston position and the geometry of the facility constitute the inputs to the model.

First, the compression in the tube is investigated when the downstream shutter valve is closed (see sketch in Figure 2). The assumptions of lightweight piston and absence of friction are made.

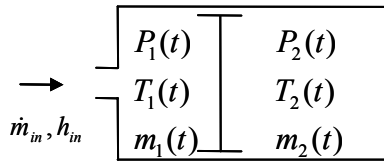


Figure 2: Compression tube before shutter opening

In each of the volumes 1 and 2, mass and energy balances are applied and the perfect gas equation is used. At any time, an equal pressure is assumed on both sides of the piston:  $P_2 = P_1$ . To solve these equations, an iterative procedure is adopted based on two logical steps.

In the first step, a mass  $\Delta m_1$  is injected in the volume but the piston is not allowed to slide. The corresponding pressure and the temperature rise in volume 1 can be computed with:

$$\Delta m_1 = m_1^i - m_1^{i-1} = \dot{m}_{in}^{i-1} \Delta t \quad \text{mass conservation}$$

$$m_1^i u_1^i - m_1^{i-1} u_1^{i-1} = \dot{m}_{in}^{i-1} h_{in}^{i-1} \Delta t \quad \text{energy conservation}$$

$$u^i = c_v T^i, \quad h^i = c_p T^i$$

$$P_1^i V_1^i = m_1^i R T_1^i \quad \text{perfect gas equation}$$

With  $x^{i-1} = \frac{\Delta m_1}{m_1^{i-1}}$ , one has:

$$T_1^i = T_1^{i-1} + \frac{x^{i-1}}{1+x^{i-1}} (\gamma T_{in}^{i-1} - T_1^{i-1})$$

The corresponding pressure can be calculated with the perfect gas equation.

In the second step, no mass is admitted in the cylinder but the piston is allowed to slide by small successive displacements  $\Delta z$ . After each displacement, the pressure and temperature are computed in each volume according to an isentropic evolution:

$$\frac{P_1^i}{P_1^{i-1}} = \left( \frac{V_1^{i-1}}{V_1^i} \right)^\gamma \quad \text{and} \quad \frac{T_1^i}{T_1^{i-1}} = \left( \frac{P_1^i}{P_1^{i-1}} \right)^{\frac{\gamma-1}{\gamma}}$$

The displacement is stopped when the two pressures on each side of the piston are equal. Note that this method allows having non-constant inlet mass flow  $\dot{m}_{in}$ . When the wanted stage inlet pressure is reached downstream of the piston, the shutter can be opened.

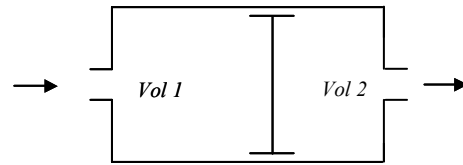


Figure 3: Compression tube model after shutter opening

### After shutter opening

#### - Shutter valve opened

The linear displacement of the shutter valve is measured and the corresponding area evolution is used to describe the progressive opening of the valve (see Figure 4).

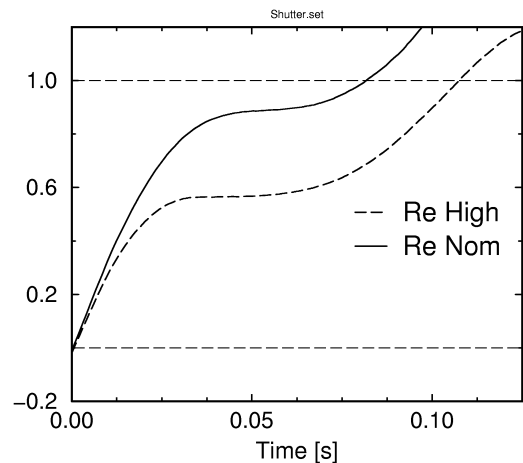


Figure 4: Dimensionless area change as a function of time from measurements for Re nom and Re high conditions.

As soon as the shutter valve starts to open, the flow enters the settling chamber and the test section. They are filled progressively until the downstream sonic throat becomes choked.

The set of equations applied on the open volume 1 can now be applied to the open volume 2 with a tube exiting mass flow  $\dot{m}_{out}$ . Coolant and leakage flows are also included in the model as sketched in Figure 5. The iterative method described above is used to progress in time.

When the shutter is fully opened, the pressure in volume 2 remains constant if the tube incoming and exiting volumetric flow rates are equal. As the downstream throat is choked, constant conditions are maintained in the test section. Note that the entering and exiting tube mass flows  $\dot{m}_{in}$  and  $\dot{m}_{out}$  are different because of the different densities in the volume 1 and 2.

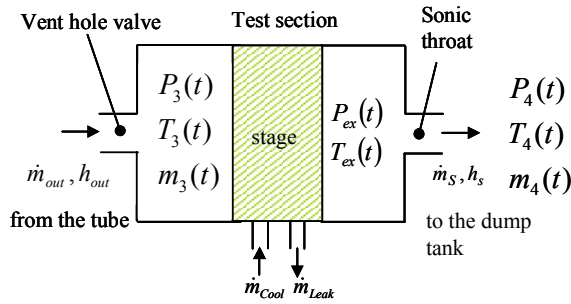


Figure 5: Settling chamber and test section model

The balances of the internal energy and incoming/outcoming enthalpies in the settling chamber (see Figure 5) can be expressed as:

$$m_3^i - m_3^{i-1} = \dot{m}_{out}^{i-1} \Delta t - \dot{m}_s^{i-1} \Delta t + \dot{m}_{Cool}^{i-1} \Delta t - \dot{m}_{Leak}^{i-1} \Delta t$$

$$m_3^i u_3^i - m_3^{i-1} u_3^{i-1} =$$

$$\left[ \dot{m}_{out}^{i-1} h_{out}^{i-1} - \dot{m}_s^{i-1} h_s^{i-1} + \dot{m}_{Cool}^{i-1} h_{Cool}^{i-1} - \dot{m}_{Leak}^{i-1} h_{Leak}^{i-1} \right] \Delta t$$

With  $x_{out}^{i-1} = \frac{\dot{m}_{out}^{i-1} \Delta t}{m_3^{i-1}}$ ,  $x_S^{i-1} = \frac{\dot{m}_s^{i-1} \Delta t}{m_3^{i-1}}$ ,  $x_{Cool}^{i-1} = \frac{\dot{m}_{Cool}^{i-1} \Delta t}{m_3^{i-1}}$ ,

$x_{Leak}^{i-1} = \frac{\dot{m}_{Leak}^{i-1} \Delta t}{m_3^{i-1}}$  one obtains:

$$T_3^i = T_3^{i-1} +$$

$$\frac{\gamma (x_{out}^{i-1} T_{out}^{i-1} + x_{Cool}^{i-1} T_{Cool}^{i-1} - x_{Leak}^{i-1} T_{Leak}^{i-1} - x_S^{i-1} T_S^{i-1}) - T_3^{i-1}}{1 + x_{out}^{i-1} + x_{Cool}^{i-1} - x_{Leak}^{i-1} - x_S^{i-1}}$$

The corresponding pressure can be calculated with the perfect gas equation.

Of course, the mass flow that exits the vent hole must be calculated in order to be able to progress in time.

### Vent hole valve mass flow

When the shutter valve starts to open, the total pressure in the settling chamber is still equal to the initial pressure i.e. about 50 mbar. The ratio between  $P_2$  and the static pressure in the vent hole  $P_{sv}$  is greater than the critical pressure ratio (1.879) and thus the section of the vent hole valve is choked. For choked conditions, the mass flow can be calculated using only the upstream total conditions with:

$$\dot{m}_{out} = \frac{P_2 A_V(t)}{\sqrt{T_2}} \sqrt{\frac{\gamma}{R} \left( \frac{2}{\gamma+1} \right)^{\frac{\gamma+1}{\gamma-1}}}$$

It is reminded that the vent hole valve area is a function of time.

As the settling chamber is filled-up, the static pressure in the vent hole  $P_{sv}$  rises. When the ratio  $P_2/P_{sv}$  becomes smaller than the critical pressure ratio, the section of the shutter valve gets unchoked and the knowledge of the velocity across the vent hole (and thus of the static pressure  $P_{sv}$ ) is required to compute the mass flow. For this purpose, the value of  $P_{sv}$  is artificially coupled to the total pressure in the settling chamber through:

$$P_2^i - P_{sv}^i = \Delta P_{sc} - \Delta P_{TS}^i$$

where :

- $\Delta P_{TS}^i$  is the difference between the total pressure in the tube and the total pressure in the settling chamber,

- $\Delta P_{sc}$  is the difference between the total pressure in the tube and the static pressure in the section of the shutter valve when steady conditions are reached. A first guess of this value is made and, once the mass flow is derived, this assumption is validated. Once the evolution of the static pressure  $P_{sv}$  is known, all the other conditions in the vent hole can be calculated and the mass flow  $\dot{m}_{out}$  is derived with:

$$\dot{m}_{out} = \rho_v V_v A_v = \frac{P_{sv}}{RT_{sv}} A_v M_v \sqrt{\gamma R T_{sv}}$$

### Turbine Stage

In reality, there are total pressure and temperature losses between the vent hole valve and the turbine stage inlet (about 10% for both pressure and temperature). Pressure losses are due to the sudden enlargement in the settling chamber and the presence of two successive rows of grids inside the settling chamber. The temperature loss is simply due to the heat exchange between the hot

compressed gas and the cold endwalls of the rig. This is taken into account introducing loss coefficients. As a result, when steady state conditions are reached, the tube pressure and temperature are higher than the stage inlet conditions.

Even during the transient phase, the turbine stage is assumed to operate with a constant pressure ratio and a constant efficiency. This allows to compute the turbine exit conditions  $P_{ex}$ ,  $T_{ex}$ :

$$P_{ex} = \frac{P_3}{\pi}$$

$$T_{ex} = T_3 \left[ 1 - \eta \left( 1 - \pi^{\frac{1-\gamma}{\gamma}} \right) \right]$$

### Sonic throat mass flow downstream dump tank

The mass flow in the downstream throat is computed exactly in the same way than the vent hole mass flow. The only difference is that in this case, the throat is initially unchoked and then becomes choked. Because the throat becomes choked very quickly, the choking criterion was based directly on a ratio of total pressures  $P_{ex}/P_4$  for simplicity.

To compute the evolution of pressure and temperature in the dump tank, mass flow and energy balances are applied to the closed volume in a similar way to what was done for volume 1 of the upstream cylinder.

### Automatic fitting of the experimental data

In the model described previously, the tube inlet mass flow  $\dot{m}_{in}$  and the downstream throat area  $A_S$  must be known. These parameters can be obtained by matching the calculated tube total pressure increase with the one measured in the volume 2. Figure 6 shows the behaviour of the tube pressure as a function of time.

When the shutter is closed, the pressure increases quasi linearly (part A). The rate of increase depends only on the volumetric flow rate entering the tube, i.e. on the tube inlet mass flow  $\dot{m}_{in}$  and temperature. Assuming that the air is entering at ambient temperature, a value  $\dot{m}_{in}$  of the inlet mass flow can be found in such a way that the model reproduces the measured evolution. Owing to the large expansion of the air when it enters the cylinder (the pressure of the supply reservoir is of the order of 250 bar) the temperature of the air is not well known. As a result, the value of  $\dot{m}_{in}$  is probably not representative. This does not affect the quality of the values that are determined downstream of the piston because what is

important is to have the correct volumetric flow rate.

The second part of the signal (after the shutter opening, B in Figure 6) is depending on the sonic throat area downstream of the turbine stage. This area is determined by matching the calculated pressure slope with the experimental signal in part B. If the pressure decreases, this means that the throat area is too large to maintain constant conditions. If it increases, the throat area is too small. When the throat area is well matched with the cylinder inlet conditions, the mass flow in the test section is constant. Note that, due to coolant and leakage flows, the mass flow that enters the test section is different from the mass flow that exits the test section.

In order to apply the model to a large number of tests, it was implemented inside an iterative loop that modifies automatically the inlet tube mass flow and the downstream throat area until the predicted tube pressure increase matches the experimental one.

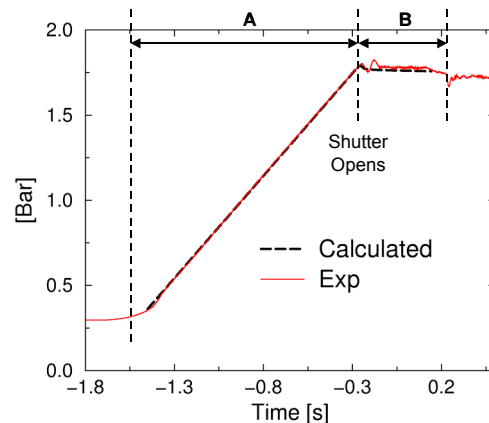


Figure 6: Total tube pressure as a function of time

### VALIDATION AGAINST EXPERIMENTAL DATA

The model is applied to a number of tests with different test conditions. Examples of results are shown in Figure 7 for the *Re Nom*, *P/p Nom* condition. In practice, the throat area sets the pressure ratio of the stage. When the wanted pressure ratio is achieved, the area of the valve that controls the tube inlet mass flow is adjusted to obtain matching conditions. The value of this area also depends on the current pressure inside the supply reservoir. Depending on the accuracy of the inlet valve area adjustment, some of the tests are well matched while for others, the pressure during the blowdown increases or decreases slightly and thus the mass flow is not exactly constant. What is remarkable in Figure 7 is that once the downstream throat area has been determined by fitting one of the tests, all the other tests can be fitted accurately

with this same area by changing only the tube inlet mass flow  $\dot{m}_{in}$ . This means that the model is able to resolve test-to-test variations and provides an accurate value of the mass flow for each test.

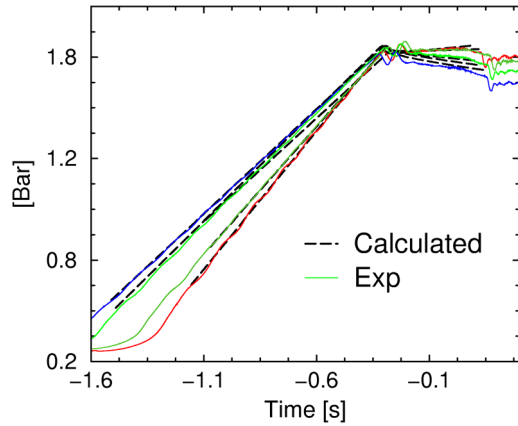


Figure 7: Total tube pressure for different tests

The large dispersion in the tube pressure increase during the compression phase A, and consequently the non-perfect matching conditions, has a little influence on the stage mass flow during the blow-down. This is due to the fact that, whatever is the tube inlet mass flow  $\dot{m}_{in}$ , the shutter valve always opens when a given pressure level is reached. Hence the mass flow at the time of the shutter opening is always the same and does not depend if the matching is good or not. Afterwards, the tube pressure may rise or decrease depending on the matching and, because of the short test time, this increase/decrease is rather limited. As a result, the large dispersion observed in the tube inlet mass flow  $\dot{m}_{in}$  does not cause a large variation of the stage mass flow  $\dot{m}_s$  during the blowdown.

The predicted piston displacement law is shown in Figure 8 for two different operating conditions. The piston speed decreases during the compression phase and stays constant after the shutter opening. The lower lines represent the experimental and calculated signal from an optical probe that detects the piston passage just before it reaches the extremity of the tube. The agreement is satisfactory and hence the assumption of an isentropic compression can be considered reasonable. Indeed, if the efficiency of the compression was far from 1, the predicted and measured displacement laws would be different.

Another information that can be extracted is the maximum possible testing time that is the time the piston needs to reach the end of the cylinder after the shutter opening. The test time is smaller in *Re High* conditions because of the higher piston velocity required to provide a larger mass flow (the *Re high* conditions is achieved by increasing the

stage inlet pressure at constant stage pressure ratio, thus the mass flow is higher).

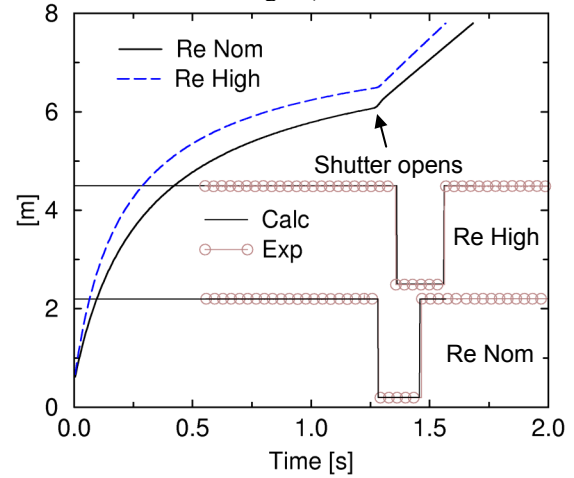


Figure 8: Piston displacement and detection as a function of time.

Figure 9 and Figure 10 show the settling chamber pressure and temperature evolutions as a function of time. The transient phase and the test duration are reasonably well predicted while the steady pressure level results from the loss coefficient applied between the vent hole and the stage inlet.

The predicted temperature peak in Figure 10 is due to the sudden compression of the air in the settling chamber that dominates the mixing with the incoming air during the transient phase. At *Re nom*  $P/P_{nom}$ , the initial pressure ratio between the tube and the settling chamber is  $1.620/0.050=32$ . An isentropic compression in a closed volume with this pressure ratio would multiply the initial temperature by 2.7 i.e.  $300 \times 2.7=810$  K. When the downstream throat gets choked, the compression stops and the gas is cooled down by the colder (440 K) incoming air. Thermocouple measurements show smaller increases but this can be attributed to their limited frequency response. Larger peaks were observed when measuring with a cold wire that has a much higher frequency response. Unfortunately, such measurements are not available at the stage inlet. The *Re High* conditions presents two peaks probably due to the shape of the shutter opening law.

The behavior of the vent hole mass flow  $\dot{m}_{out}$  and sonic throat mass flow  $\dot{m}_s$  are presented in Figure 11 and Figure 12 for *Re Nom* and *Re High* conditions. Under steady condition, the difference between the vent hole and the sonic throat mass flows is due to the coolant stage mass flow and leakage mass flow. The behavior of the mass flow

during the transient time is strongly affected by the shutter opening law.

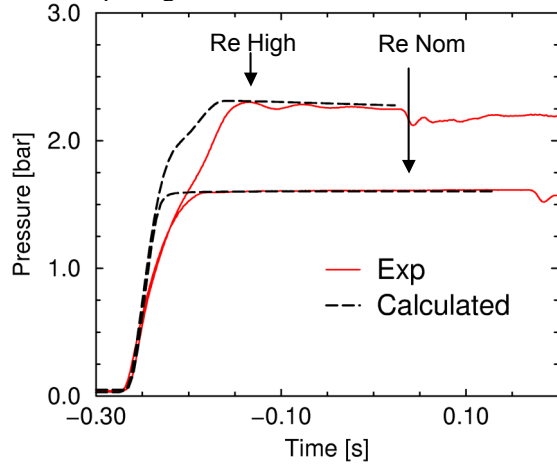


Figure 9: Total pressure evolution in the settling chamber.

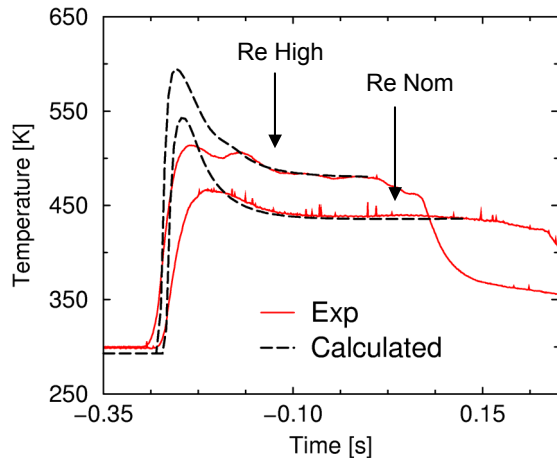


Figure 10: Total temperature evolution in the settling chamber.

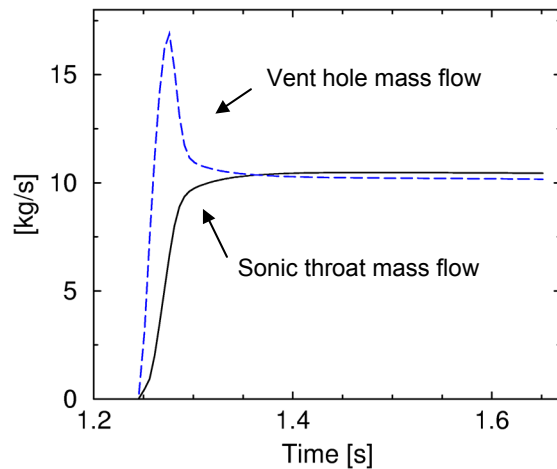


Figure 11: Mass flows in Re Nom condition

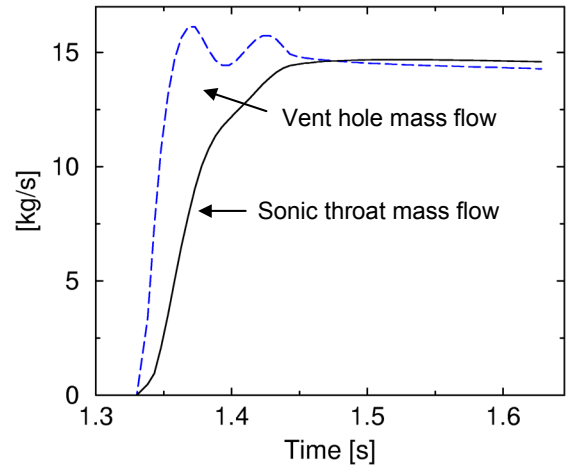


Figure 12: Mass flows in Re High condition

### UNCERTAINTY ANALYSIS

The uncertainty on the mass flow is computed according to Kline & McClintock (1953):

$$\Delta \dot{m}_s = \sqrt{\sum_{j=1}^N \Delta \dot{m}_j^2} \quad (7)$$

where  $\Delta \dot{m}_j$  is the variation of the mass flow caused by the variation of the parameter  $i$  by an amount equal to the uncertainty on this parameter. The contributions of the different parameters to the overall uncertainty are listed in Table 2 for the *Re nom P/P nom* case.

Parameter	Uncertainty	$\dot{m}_s$	$\Delta \dot{m}_s$
Tube pressure	+/- 20 mbar	10.524	0.195 %
Ambient temperature	+/- 1 K	10.524	0.195 %
Initial tube pressure	+/- 5 mbar	10.538	0.32 %
Shutter valve trigger	+/- 1.4%	10.541	0.36 %
Coolant mass flow	+/- 1%	10.505	0.013 %
Area detection	+/- 1%	10.568	0.61 %
Tube volume	+/- 1 mm	10.518	0.13 %

Table 2: Uncertainty due to each parameter

The overall uncertainty is equal to 0.88 %. The analysis shows that the critical quantity is the sonic throat area. As mentioned before, this parameter results from the fitting of the total tube pressure after the shutter opening. Hence the “quality” of the pressure signal is particularly important for an accurate fitting of the signal. Figure 13 and Figure 14 show the tube total pressure behavior for *Re Nom* and *Re High* conditions. For the *Re Nom* condition, the tube pressure stays quite constant. For *Re High* conditions, oscillations are observed. As a consequence, the fitting is affected by a larger uncertainty than for *Re Nom*.

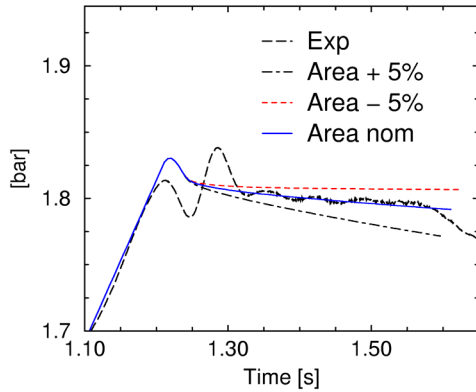


Figure 13: Tube total pressure during the blowdown for *Re Nom* condition.

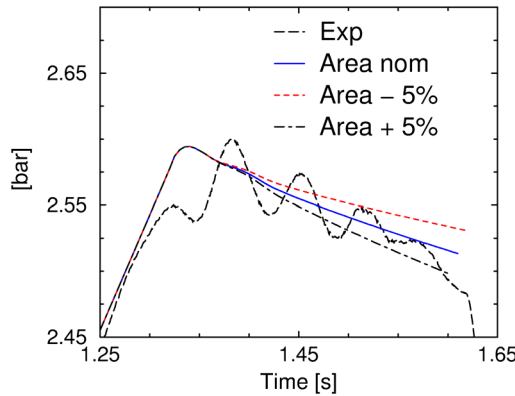


Figure 14: Tube total pressure during the blowdown for *Re High* condition.

## MASS FLOW DETERMINATION

### Stage mass flow from the model

Stage mass flow results are presented in Table 3, together with the relative uncertainty and test-to-test dispersion.

The large dispersion observed for the *Re Nom* conditions is caused by the large dispersion in the tube total pressure slope. In this case, the matching condition is not completely fulfilled for each test and the stage mass flow has not always the same value. This proves that the model is able to resolve test-to-test variations. The final uncertainty is satisfactory. For the *Re High* condition (1 and ½ stage), the dispersion is smaller owing to the almost constant inlet compression tube mass flow  $\dot{m}_m$ . This can be explained by the different inlet compression duct supply configuration. For the *Re High* condition, two ducts and an adjustable valve supply the mass flow, while for the *Re Nom* condition, only one duct and the adjustable valve are used. As a result, the mass flow  $\dot{m}_m$  is more influenced by the valve settings for *Re nom* than for *Re high*. The uncertainty is almost doubled with respect to the *Re nom* case. As

mentioned earlier, this is due to the oscillations in the tube pressure after the shutter opening that limit the quality of the fitting. The repeatability being better than the uncertainty, this uncertainty will be mostly systematic. This means that the mean value of the mass flow may be systematically over or under predicted but variations below the uncertainty (but above the repeatability) can be resolved.

<u>Single stage configuration</u>	<u>Stage mass flow [kg/s]</u>
<i>Test conditions</i>	
Re Nom P/p Nom [kg/s]	10.55
Re Nom P/p Low [kg/s]	10.1
<i>Uncertainty</i>	+/- 0.88 %
<i>Dispersion</i>	+/- 2.86 % (20:1)
<u>1 and ½ stage configuration</u>	
0% rotor cooling	15.27
2% rotor cooling	15.35
3% rotor cooling	15.36
<i>Uncertainty</i>	+/- 1.6 %
<i>Dispersion</i>	+/- 0.40 % (20:1)

Table 3: Mass flow computation results, uncertainty, dispersion

### Stage mass flow from area traverses

For comparison purpose, the stage mass flow can also be computed by integrating the stage exit velocity field over the annular exit area:

$$\dot{m}_s = \iint_{\text{Surface}03} \frac{P_{ex}}{RT_{ex}} M_{ex} a_{ex} \cos \alpha_{ex} Ads$$

where  $a_{ex} = \sqrt{\gamma RT_{ex}}$

The velocity vector was computed from stage downstream measurements of total pressure, static pressure, total temperature and flow angle (see Figure 15). The results of the uncertainty analysis for *Re nom P/P nom* are reported in Table 4.

It appears clearly that the uncertainty on the stage mass flow is of the same magnitude than the uncertainty on the total pressure. To improve the accuracy close to the endwalls, the dimensionless pressure profile resulting from a 3D N-S computation was used. Indeed, the 5 holes probe does not allow to perform measurements closer than 1.7 mm from the endwalls (5 holes probe head diameter: 3.2 mm). The stage mass flow results for the *Re nom P/P nom* condition are presented in Table 5. The mean values of the mass flow are slightly different from the values calculated with the CT3 model but they agree within the uncertainty bandwidths. This method is less accurate (uncertainty of 3.85%). Moreover, the stage downstream profiles require performing several tests. This mean that, in addition of the



accuracy on each quantity, the final profile also suffer from the quality of the test-to-test repeatability.

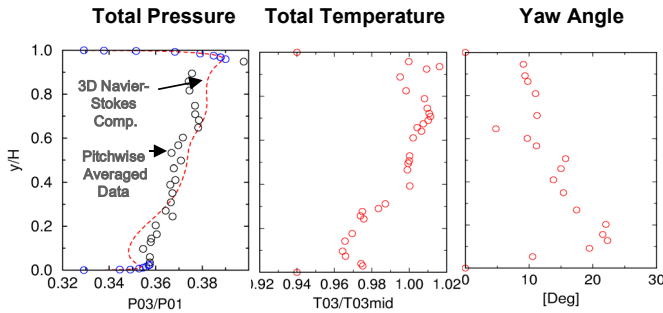


Figure 15: Stage downstream pressure, temperature and flow angle measurements.

Parameters	Uncertainty	$\Delta \dot{m}_s$	$\Delta \dot{m}_s \%$
$P_{0ex}$	0.83 %	0.4013	3.81
$T_{0ex}$	0.85 %	0.0469	0.44
$P_{ex}$	1.51 %	0.01	0.094
$a_{ex}$	6 %	0.03	0.284
$P_{0ex}$ B.L	1 %	0.0211	0.19
	Sum	0.4147	3.85

Table 4: Uncertainty analysis when using the pitch-wise averaged data to compute the stage mass flow (*Re nom P/P nom*)

Single stage configuration	Stage mass flow [kg/s]
Test conditions	
Re Nom P/p Nom [kg/s]	10.54
Re Nom P/p Low [kg/s]	10.52
Uncertainty	+/- 3.85 %

Table 5: Pitch-wise averaged method mass flow results.

## CONCLUSIONS

An unsteady modelisation of the CT-3 compression tube test rig is carried out. The method consists in mass flow and energy balances applied to each volume of the test rig at each time step. The measured shutter valve opening law is used for more accuracy. Isentropic relationships are used but total pressure and total temperature losses in the settling chamber are taken into account using simple loss coefficients based on measurements results. The mass flow history is computed in two locations: the shutter valve vent hole and the stage downstream sonic throat.

The model is able to reproduce very accurately the behavior of the rig. Comparison with measured tube total pressure increase shows that even small test-to-test variation can be resolved. The piston displacement is also well predicted. This validates the use of isentropic relationship during the compression phase. In addition, the model can be used to predict the blowdown duration depending

on the wanted test conditions. In a more general way, it could be used to design a compression tube facility.

The transient evolution of pressure and temperature in the test section is also compared with the experimental data and a good agreement is obtained. The overshoot in the temperature is due to the sudden compression of the air that dominates the mixing with the incoming air during the transient phase.

Finally, the model is used to fit the tube pressure history for a number of tests and the corresponding mass flows are evaluated. In single stage configuration (*Re nom*), the uncertainty on the mass flow is small (+/- 0.88%) but the test-to test dispersion is large (+/-2.86%) due to the difficulty of adjusting the rig inlet mass flow to obtain constant conditions during the blowdown.

In the one and a half stage configuration (*Re high*), the uncertainty is larger (+/- 1.6%) due to oscillations in the tube total pressure during the blowdown that affect the quality of the fit. However, the test-test dispersion is smaller than the uncertainty (+/-0.4 %) . This means that a part of the uncertainty is due to systematic errors but mass flow variations between 0.4% and 1.6% can be resolved.

## REFERENCES

- Dénos, R., Arts, T., Paniagua, G.- Michelassi, V., and Martelli, F., 2001, "Investigation of the Unsteady Rotor Aerodynamics in a Transonic Turbine Stage", *Journal of Turbomachinery*, Vol. 123, no 1, pp. 81-89.
- Guenette, G.R., Epstein, A.H., Ito, E., 1989 "Turbine Aerodynamic performance measurements in a short duration facilities" AIAA/ASME/SAE/ASEE 25<sup>th</sup> Joint Propulsion Conference, Monterey, CA.
- Jones, T.V., Schultz, D.L., and Hendley, A.D., 1973, 'On the Flow in an Isentropic Light Piston Facility', Reports and Memoranda no 3731, Dept. Engineering and Science, University of Oxford.
- Keogh, R. C., Guenette, G. R., Sommer, T. P., 2000, "Aerodynamic performance measurements of a fully-scaled turbine in a short duration facility", *ASME paper 2000-GT-486*.
- Kline, S. J., McClintock, F. A. 1953 "Describing uncertainties in single sample experiments" *Mechanical Engineering*, Vol. 75, No 1.
- Sieverding, C.H., and Arts, T., 1992, "The VKI compression tube annular cascade facility CT3". ASME Paper 92-GT-336.